Intumescent polypropylene: reaction to fire and mechanistic aspects

Serge Bourbigot*[1], Johan Sarazin[1], Tsilla Bensabath[1], Fabienne Samyn[1] and Maude Jimenez[1]

[1]R_2Fire group/UMET – UMR CNRS 8207, ENSCL, University of Lille, France

Corresponding author: serge.bourbigot@ensc-lille.fr

ABSTRACT

The concept of intumescence was applied to make flame retarded polypropylene (PP). This paper examines two types of intumescence in PP based on expandable graphite (EG, physical expansion) and on modified ammonium polyphosphate (AP760, chemical expansion). Reaction to fire of PP containing EG and AP760 was first evaluated by cone calorimetry. The incorporation of intumescent additives at relatively low loading (10 wt%) in PP permits the reduction by 70% of peak of heat release rate (pHRR). The mode of action occurs via the formation of an expanded carbonaceous layer in all cases. The protective coating acts mainly as heat barrier in the case of the formulations containing AP760 or as heat dissipater with EG. The incorporation of small amount of EG in PP-AP760 modifies heat transfer in the coating creating a strong anisotropy. Upon expansion, graphite worms align normal to the surface increasing the transverse heat conductivity (lower efficiency of the heat barrier) and hence, decreasing the fire performance (decrease by only 30% of pHRR). Kinetic analysis was then performed to quantify the thermal stability of the intumescent systems. It reveals that the intumescent additives do not modify the reactional scheme of the PP thermal decomposition but they increase slightly the thermal stability of the intumescent systems. For all materials, the decomposition model follows a reactional scheme at two successive reactions. This model was determined in dynamic conditions (conditions of thermogravimetry with linear heating rates) but it is able to simulate the decomposition of the materials in isothermal conditions (excellent agreement between the simulated and experimental curves).

KEYWORDS:

Intumescence; polypropylene; kinetic analysis; heat transfer

INTRODUCTION

Economical manufacturing methods for mass production and improvements of properties of finished products have in many applications greatly contributed to replace traditional materials like metals or wood with plastics and rubbers. In particular, polypropylene (PP) is the fastest growing commodity plastic worldwide. It has found its place in many sectors such as building, transportation (automotive, railways …), electrical engineering (electrical / household appliances, housings …) or paper industry.

The use of the organic polymer systems like PP, which are flammable, leads to greater fire risks and thus to growing importance of flame retardancy [1]. Some events have shown the need to improve fire resistance. As an example, the PP fire at the BASF plant (March 1995 in Teeside, UK) which has been described as one of the largest fires ever seen in the UK during the peacetime (more than 10,000 tons of PP were consumed) [2]. This clearly entails a more comprehensive appraisal of all aspects of the combustion of polymers and the ways to prevent it. The high carbon and hydrogen content of PP

(like many other synthetic polymers) makes it combustible. To enable PP to participate and perform safely, flame-retardants are added in applications where regulatory or specifications require an enhanced flame retardant capability over and above the unmodified polymer. The flame retardant will not make the resulting compound non-combustible. It will however make the material more ignition resistant. During burning, the sufficiently flame retarded plastic will reduced the flame spread time over that of unmodified PP. Flame retardants exert many different modes of action as a function of the chemical nature of the polymer-flame retardant systems and of the interactions between the components. It is considered that inhibition of burning is achieved by modification of either the condensed phase or the dispersed or gaseous phase in a physical and/or chemical mode [3].

The motivation of this paper is to examine the flame retardancy of PP using the concept of intumescence (mode of action in the condensed phase). When heated beyond a critical temperature, an intumescent material begins to swell and then to expand. The result of this process is a foamed cellular charred layer on the surface, which protects the underlying material from the action of the heat flux or the flame. Visually, the swelling and the expansion looks like 'black waves' swollen at the surface of the material and the final char exhibits hemispheric shape with a roughed or smooth surface. The concept of intumescence enables to make flame retarded polymeric materials (including PP-based materials) exhibiting high performance [4]. Typically, the ingredients of intumescence are mainly composed of an inorganic acid or a material yielding acidic species upon heating (e.g. phosphate), of a char former (e.g. pentaerythritol) and of a component that decomposes at the right temperature and at the right time to enable the expansion of the system (e.g. melamine). Those types of ingredients were incorporated in PP in the 80s and 90s and gave high limiting oxygen index (LOI) and low heat release rate (HRR) [5, 6]. More sophisticated flame-retardants combining the ingredients' triplet in all in one molecule and made from organic syntheses were designed but they provided similar performance as the conventional formulation [4, 7-9]. Incorporation of additional filler in an intumescent PP can also involve synergistic effects. Performance is enhanced dramatically adding small amount of an additional compound [7, 10-12]. Numerous synergists (micro- and nanofillers) have been used in conventional "three-based ingredients" intumescent formulations. It includes the boron compounds (zinc borates, B_2O_3, borophosphate, borosiloxane), phosphorus compounds (phosphazene, $ZrPO_4$), silicon compounds (silica, silicone, silicalite), aluminosilicates (mordenite, zeolite, montmorillonite), rare earth oxides (La_2O_3, Nd_2O_3), metal oxides (MnO_2, ZnO, Ni_2O_3, Bi_2O_3, TiO_2, ZrO_2, Fe_2O_3) and others (carbon nanotubes, silsesquioxanes, layered double

hydroxides, Cu, Pt, talc, sepiolite, zinc and nickel salts). The presence of this additional filler can modify the chemical (reactivity of the filler versus the ingredients of the intumescent system) [13] and physical (expansion, char strength and thermophysical properties) [14] behavior of the intumescent char when undergoing flame or heat flux leading to enhanced performance.

This short survey on intumescent PP shows that the method to develop the intumescence phenomenon is mainly based on series of chemical reactions occurring timely. Another way to make intumescence in a polymeric matrix is the physical expansion. In other words, the rapid sublimation of a molecule (and/or the decomposing products) creates the expansion of the top degraded layer of the polymer to make an intumescent coating. This mechanism occurs when using expandable graphite (EG). EG is a synthesized intercalation compound of graphite that expands or exfoliates when heated. A wide variety of chemical species can be used to intercalate graphite materials (e.g. sulfate, nitrate, various organic acids …) [15]. It was applied in PP in combination with conventional intumescent ingredients [16, 17]. The mechanism involved was investigated in some aspects (chemistry of the system) but it remains poorly understood. It is the purpose of this work to revisit the mode of action of physical intumescence in PP and to make comparisons with chemical intumescence.

This paper examines two types of intumescence in PP based on EG (physical expansion) and on modified ammonium polyphosphate (AP760, chemical expansion). Some examples of using ammonium polyphosphate and EG can be found elsewhere [18-20] but not in PP. Reaction to fire of PP containing EG and AP760 is first evaluated by cone calorimetry and the efficiency of the intumescent barrier is measured quantitatively at the same time. Kinetic analysis is then performed to quantify the thermal stability of the intumescent systems.

EXPERIMENTAL

Materials and processing

Commercial grade of PP was used in this work: PP (PPH9060) was supplied by Total petrochemicals (Feluy, Belgium). PPH9060 has a melt flow rate (MFR) for a load of 2.16 g at 230°C of 25 g/10 min.

Expandable graphite (EG) is the commercial grade ES350F5 from Graphitwerk Kropfmühl (Germany) with an average particle size of 300 µm. Sulfate was used in this grade as intercalation compound to make graphite bisulfate. Modified ammonium polyphosphate (AP760) is the commercial grade of

Clariant (Germany) with the brand name Exolit AP760. It is an intrinsic intumescent system containing 20 wt% phosphorus and 14 wt% nitrogen acting in synergy. It is mainly based on ammonium polyphosphate as acid source and tris(hydroxyethyl) isocyanurate (THEIC) as char former.

Processing

The strategy was to blend PP with flame-retardants (FRs) in a twin-screw extruder. The total loading of FRs in PP was 10 wt% varying the ratio AP760/EG (wt/wt) at 10:0; 5:5; 9:1 and 0:10. This loading was selected because it provides an acceptable performance according to cone calorimetry. Compounding was performed using HAAKE Rheomix OS PTW 16 twin-screw extruder. The extruder is a co-rotating intermeshing twin screw with a barrel length of 400 mm and screw diameter of 16 mm (L/D = 25) with 10 zones. PP and FRs were incorporated using two gravimetric side feeders into the extruder. Polymer flow rate is fixed to extrude about 500 g/h with a screw speed of 300 rpm. The temperature profile of the extruder from feeder to die was set at 200/ 200/ 200/ 200/ 200/ 170/ 185/ 180/ 200/ 200°C.

Cone calorimetry

FTT (Fire Testing Technology) Mass Loss Calorimeter (MLC) was used to carry out measurements on samples following the procedure defined in ASTM E 906. The equipment is identical to that used in oxygen consumption cone calorimetry (ASTM E-1354-90), except that a thermopile in the chimney is used to obtain heat release rate (HRR) rather than employing the oxygen consumption principle. Our procedure involved exposing specimens measuring 100 mm x 100 mm x 3 mm in horizontal orientation. External heat flux of 35 kW/m² was used to perform the experiments. This flux corresponds to common heat flux in mild fire scenario. MLC was used to determine heat release rate (HRR) and total heat release (THR). When measured at 35 kW/m², HRR is reproducible to within ±10%. The cone data reported in this paper are the average of three replicated experiments.

In addition to those measurements, a thermocouple (K-type thermocouple of 0.5 mm diameter) was embedded on the backside of the materials in horizontal position. It measured temperature as a function of time during a regular cone experiment. In this experimental set-up, it is necessary to assume that additional conductive effects due to the thermocouple are negligible.

X-ray tomography

The expanded intumescent specimens obtained after cone calorimetry were placed in X-ray µCT (computed microtomograpy) for the analysis of the inner morphology without structural damage. The resulting recordings over 360◦ were reconstructed to obtain the computerized 3D CT volumes. The tomography was performed using the microtomography setup at ISIS4D X-ray CT platform (equipped with UltraTom from RX Solutions). The set-up consisted of two X-ray tubes (micro and nano focus), a sliding and rotating stage holder, a flat panel detector (1920x1496 px-127 µm/px-0.2 to 60 frame/s), a linear detector (2560 px-200 µm/px-0.2 to 60 frame/s), a CCD camera (4000x2624 px-11.8 µm/px-up to 3.4 frame/s) and an image intensifier. Samples were placed on styrofoam holders and then mounted on the rotating stage to minimize the signal noise due to the holder. Samples were rotated by 360◦ with an angular step of 0.25◦. The subsequent tomography volumes were reconstructed from 1440 projection images produced by classical attenuation contrast technique and visualized using X-Act (from RX Solutions).

Kinetic analysis

ThermoGravimetric Analysis (TGA) was carried out using a Netzsch TG 209 F1 Libra at five heating rates (1, 2, 5, 10, 20 and 50°C/min) from 30°C to 800 °C in nitrogen flow (50 cm^3/min). Samples of exactly 10 mg ($\pm$0.3 mg) were put in open alumina pans. Typically, two replicates were run for each sample, and the average was reported. Both the onset (5% mass fraction loss) and peak mass loss rate have an uncertainty of 0.9°C (2σ). We corrected for each heating rate the buoyancy force (calibration with empty pan). Kinetic analysis and modeling of the degradation of the samples was made using an advanced thermokinetic software package developed by Netzsch Company [21]. For kinetic analysis, it is assumed that the material decomposes according to the Eq. (1):

$$A_{solid} \rightarrow B_{solid\ or\ liquid} + C_{gas} \quad (1)$$

The rate expression $d\alpha/dt$, where α is the degree of conversion, is assumed to be defined by Eq. (2):

$$d\alpha/dt = k(T).f(\alpha) \quad (2)$$

where k is the kinetic constant, $k = A.\exp(-E/RT)$ according to the Arrhenius law, A is the frequency factor, E is the activation energy and $f(\alpha)$ is the so-called “reaction model”. All reactions are assumed to be irreversible. In the case of decomposition and since the evolved gases were continuously removed by the fluid flow in the TGA chamber, this is a reasonable assumption. It is also assumed that the overall reaction (Eq. (1)) is the sum of individual reaction steps (formal or true step) with

constant activation energy, as generally accepted in chemistry. The model can then include competitive, independent and successive reactions. The equations were solved with multivariate kinetic analysis (determination of the parameter via an hybrid regularized Gauss-Newton method or Marquardt method).

RESULTS AND DISCUSSION

Reaction to fire

EG and AP760 and some of their combinations (AP760/EG at 5:5 (wt/wt) and 9:1 (wt/wt)) were incorporated in PP at 10 wt% total loading. The four formulations were evaluated by cone calorimetry at an external heat flux of 35 kW/m² and compared to neat PP (Fig. 1).

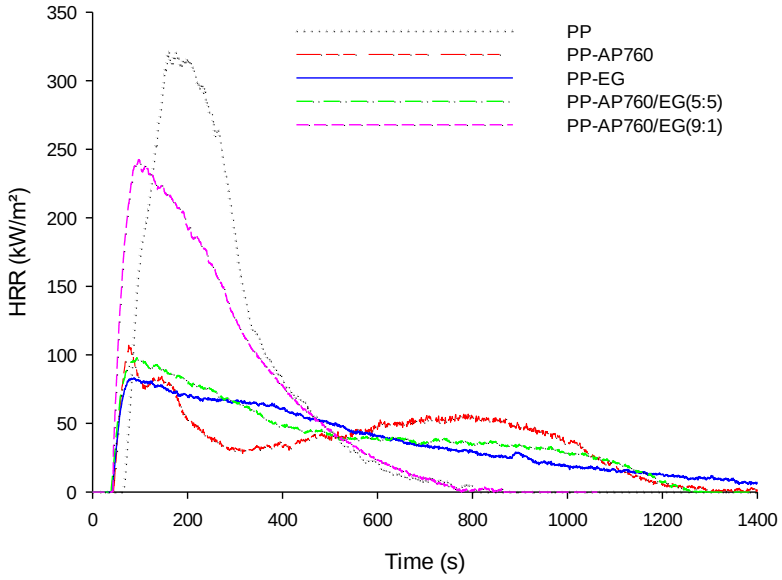

Fig. 1. HRR curves as a function of time of intumescent PP (external heat flux = 35 kW/m²)

Except for the formulation containing 1 wt% EG, the intumescent PPs exhibit peaks of heat release rate (pHRR), which are decreased by about 70%. Total heat release rate (THR) is also significantly reduced. It is decreased by about 35% for the two formulations PP-EG and PP-AP760 (82 MJ/m² *vs*. 50 MJ/m²) and by 20% for PP-AP760/EG (5:5) (82 MJ/m² *vs*. 60 MJ/m²). The formation of an expanded charred layer is observed at the surface of the materials evidencing an intumescent phenomenon (Fig. 2). The char formed from PP-AP760 is fully expanded and its surface is flat (Fig. 2 - a) but on the opposite, the two formulations PP-EG and PP-AP760/EG (5:5) exhibit an expanded 'hairy' char during the experiment (Fig. 2 – b and c). The intercalation compounds contained in EG decompose rapidly into gaseous products, which blast off the graphite flakes. Those flakes make then worms forming an entangled network at the surface of the material. This network acts as a protective layer (PP-EG, Fig.

2 – b). The combination of EG and AP760 in the formulation PP-AP760/EG (5:5) exhibits a reduced expansion compared to PP-EG. The char is also formed of entangled worms of graphite, which can be clearly distinguished at the surface (Fig. 2 – c). The relative limited expansion is probably due to the embedded graphite worms in the char increasing its viscosity. The formulation containing 1 wt% EG exhibits a pHRR only decreased by 30% and a THR decreased by 10% (82 MJ/m² vs. 70 MJ/m²). An intumescent phenomenon is also observed but its efficiency is not as high as the other intumescent PPs. The low quantity of EG in the formulation does not permit the formation of an entangled network and only graphite worms coming out of the charred surface can be observed (Fig. 2 – d). It is noteworthy the graphite worms rise up straight upon heating: they do not flatten and remain in line on the expanding char (Fig. 3).

Overall, the intumescent char formed from PP-AP760 exhibits high expansion and a smooth surface while the chars containing EG exhibit lower expansion and 'hairy' surface. It evidences therefore two distinct mechanisms: (i) the physical expansion of graphite flakes forming a protective entangled network and (ii) the formation of an intumescent char by a series of chemical reactions. Those two types of protective coating provide the same level of protection according to the cone scenario (except for the combination AP760/EG (9:1)).

(a) PP-AP760

(b) PP-EG

(c) PP-AP760/EG (5:5)

(d) PP-AP760/EG (9:1)

Fig. 2. Intumescent coatings formed from intumescent-based PP during the cone calorimetry experiment and after the ignition

Fig. 3. Charring of the formulation PP-AP760/EG (9:1) before the ignition

During the cone calorimetry experiments, thermocouples were placed on the backside of the materials to measure the temperature as a function of time and to quantify the efficiency of the intumescent barrier (thermocouple embedded in the material in horizontal position). Note all the experiments presented below are highly repeatable. It was checked the thermocouple remains at the same position before and after the experiments (no loss of contact with the matter) and hence, the measured temperature makes sense. Fig. 4 shows temperature changes as a function of time. Up to 50s, the slopes of the curves are similar and the materials heat up at about 0.5°C/s. At t>50s, the 5 curves exhibit a slope break and the temperature rise jumps to 5.2°C/s. The neat PP reduces a little bit its temperature rise at t>190s (curve of PP was stopped when the thermocouple is no longer in the matter because of the complete decomposition of PP). At t=90s, the temperature rise of PP-EG is strongly reduced at 0.6°C/s and even more at t>300s (0.15°C/s). It corresponds to the formation of an intumescent layer reducing heat transfer from the flame to the backside of the substrate and so, it limits the temperature rise on the backside. The efficiency of the intumescent chars formed by PP-AP760 and PP-AP760/EG(5:5) is less. The two curves follow the same trend as the curve of neat PP up to 150s and then their temperature rise exhibits a similar value as that of PP-EG (0.15°C/s). They reach a steady state at about 700s with similar final temperatures (520°C at 1100s). Note PP-EG does not show any steady state. It is assigned to smoldering occurring on the graphite worms (Fig. 2 – b). The higher performance of PP-EG compared to PP-AP760 and PP-AP760/EG(5:5) can be explained by the faster expansion of its intumescent coating thanks to the fast sublimation of the inserted molecules. The protective layer is therefore formed at shorter time as evidenced by the slope break at 190s and then the entangled network of graphite worms can limit the heat transfer to the bottom layer. PP-AP760/EG(9:1) exhibits an unexpected behavior because its backside temperature increases extremely rapidly to 650°C (temperature rise of 5.2°C/s). Its backside temperature reaches a pseudo steady state at 670°C for 350s (50s<t<400s) and then decreases to 545°C. This temperature drop (125°C) at 400s is unclear and it is not due to the flameout of the materials since it occurs at 660s.

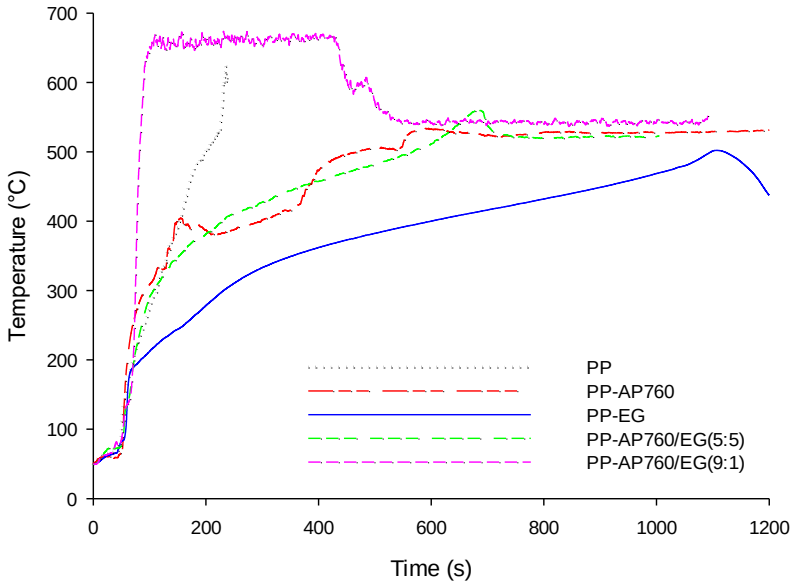

Fig. 4. Backside temperature as a function of time of intumescent PPs during cone calorimetry experiment (external heat flux = 35 kW/m²);

The temperature on the backside of PP-AP760/EG(9:1) strongly decreases after 400s while it is not observed with the other samples. To explain this, the structure of the chars was examined by X-ray tomography. The main advantage of tomography is to observe the internal structure of the samples without damaging it. The intumescent samples are brittle and it is difficult to cut them off without any modification. The cross-sections of the intumescent residues show two types of internal structures (Fig. 5). The residues of PP-AP760 and PP-AP760/EG(9:1) exhibit an expanded hollow structure with thin walls (Fig. 5 (a) and (d)). Some graphite worms can be distinguished for PP-AP760/EG(9:1) attached to the wall (Fig. 5 (d)). Note also that only a part of the sample is expanded. The residues of PP-EG and PP-AP760/EG(5:5) are also expanded but they are filled by graphite worms showing an entangled network as mentioned above (Fig. 5 (b) and (c)). The comparison of the 4 structures does not permit to explain the temperature drop occurring for PP-AP760/EG(9:1) but they confirm the comments made about the mode of protection, namely the formation of an entangled network when using EG and of an expanded charred coating when using AP760. Hence, additional experiments were performed for preparing residues stopped at characteristic times of the temperature/time curve, namely 130s (highest temperature), 460s (decreasing temperature) and 900s (end of the experiment). Because of ease, the so-prepared samples were cut off to get a rapid view of their cross-sections (Fig. 6). At 130s, the sample is relatively compact and few expanded (Fig. 6 (a)). The graphite worms are embedded in the char and are staked because of the cooling of the sample (the worms were aligned and normal to the surface during the experiment). The heat

conduction inside the solid should be high. At t = 460 s, the temperature on the backside of the sample is decreasing. Concurrently, the char is expanding creating a hollow charred coating (Fig. 6 (b)). At this time, the heat transfer is reducing and then the temperature drops down. The final residue is also a hollow coating (Fig. 6 (c)). Those observations give an explanation why the temperature decreases after a certain time: the incorporation of EG delays the expansion of the intumescent coating and hence limits the performance of the intumescent char.

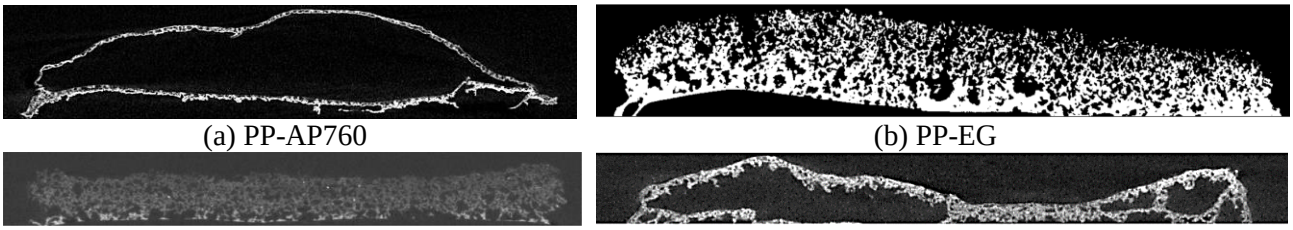

(a) PP-AP760 (b) PP-EG

(c) PP-AP760/EG (5:5) (d) PP-AP760/EG (9:1)

Fig. 5. X-ray tomography images of cross-section of intumescent coatings obtained after cone calorimetry

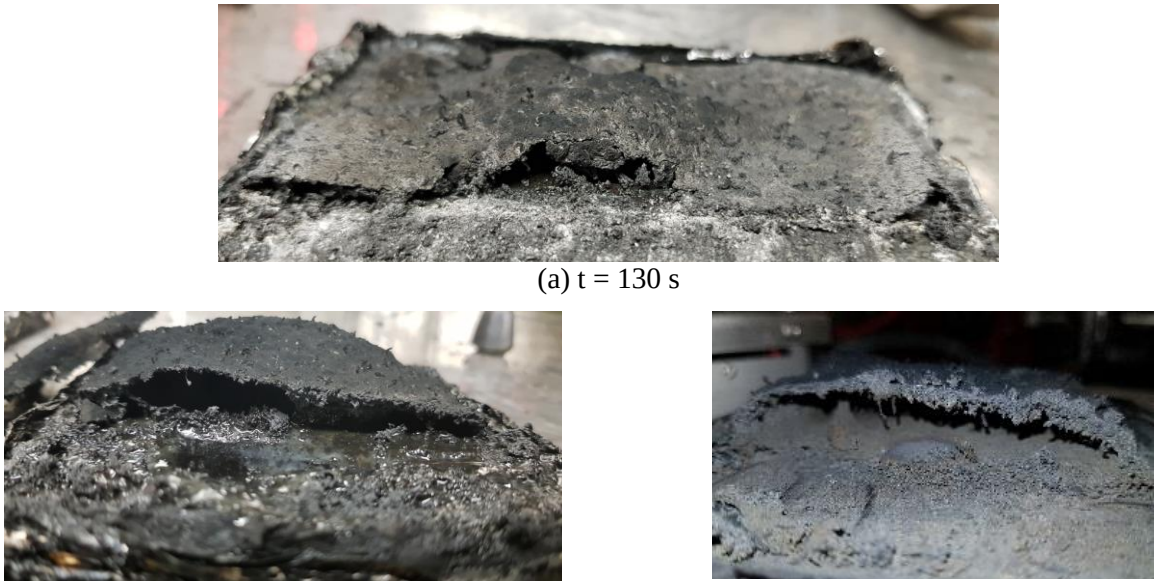

(a) t = 130 s

(c) t = 460 s (d) t = 900 s

Fig. 6. Optical images of cross-section of PP-AP760/EG (9:1) intumescent coatings prepared at different characteristic times

The results suggest the involvement of different mechanisms. PP-A760 forms an expanded char at the surface, which reduces the heat transfer from the flame to the material. The incorporation of small amount of EG in a conventional intumescent system (PP-AP760) strongly affects its performance. Visual observation shows graphite worms grows up at the surface but there is no

entanglement of the worms (Fig. 3). The worms exhibit an alignment normal to the surface and hence, they might enhance heat conductivity (transverse heat conductivity) through the material as shown by temperature measurement (see the cartoon of Fig. 7). In the other cases, EG can form an entangled network, which flattens because of the expansion. Hence, in-plane heat conductivity is enhanced (parallel to the surface) and the worms play the role of heat dissipater (this effect is limited when EG is combined with AP760). Even if the cone heater irradiates the whole surface, it is reasonable to assume heat dissipation occurs on side surfaces of the samples. Those two types of behaviour leads to huge difference in terms of performance and it evidences the anisotropic character of EG when used as FR.

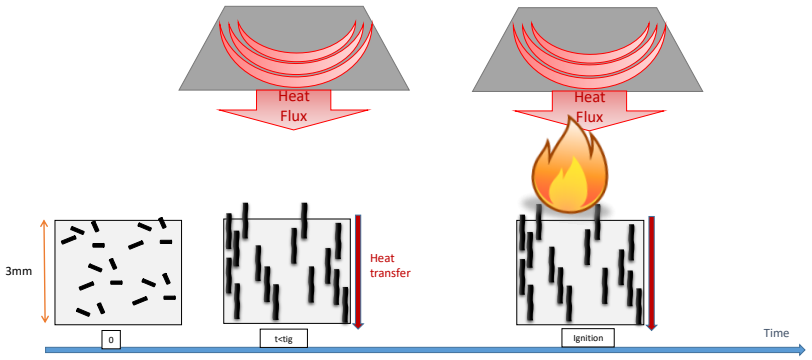

Fig. 7. Schematic description of the effects of graphite worms in PP-AP760/EG (9:1) on heat transfer through the charred network.

Kinetic analysis

The previous section has shown the fire performance of PP was strongly enhanced incorporating AP760 and EG. The goal of this section is to examine whether the thermal stability of the intumescent PPs could be modified. Fig. 8 shows TG curves of the intumescent PPs compared to neat PP. All materials exhibit a single apparent step of degradation but only the intumescent PPs have residues at high temperature (about 4.5 wt.-% for PP containing AP760 and 7.5 wt.-% for PP-EG). It is easily explained by the charring of the samples due to the intumescent ingredients. It is noteworthy PP-EG gives higher char yield than the others probably because of the high thermal stability of graphite. The onset temperature of decomposition of PP materials containing AP760 is slightly lower than that of neat PP (365°C vs. 390°C) while it is the contrary for PP-EG: its onset temperature of decomposition is at 415°C. The curves of AP760 containing PPs are superimposed and no difference can be distinguished. At T > 430°C, the thermal stability of those materials become higher than that of neat PP while it is always the case for PP-EG.

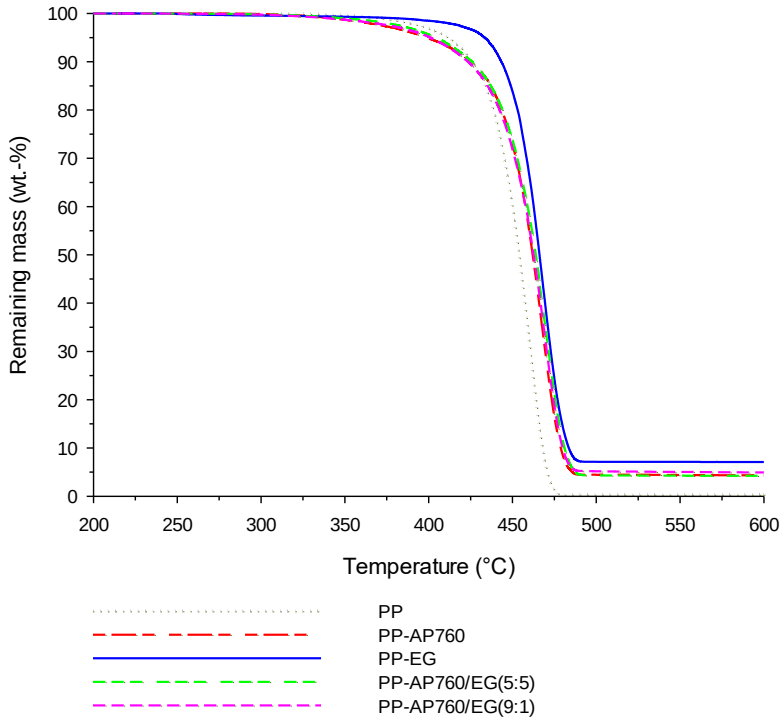

Fig. 8. TG curves of intumescent PPs compared to neat PP (heating rate = 10 K/min; nitrogen flow)

The comparison of the thermal stabilities of the PP-based materials only brings information on the temperature range where the material decomposes but it does not give any physical parameter. The approach was then to perform kinetic analysis on the thermal decomposition of the neat PP and of the 4 intumescent formulations to get kinetic parameters, namely the triplet including the frequency factor (A), the activation energy (E) and the reaction order (n). Before starting any fitting procedure, it is necessary to define a model (combination of reactions) and to preset starting values for the kinetic parameters. A convenient approach is to use model-free analysis as a preliminary step of the kinetic analysis. A model-free analysis provides the plot of the activation energy versus the conversion degree. For the 5 materials, it reveals that the plot of activation energy exhibits a pseudo-plateau at conversion degree within the range 0.2 – 0.9 between 180 and 270 kJ/mol and a more complicated shape at low and high conversion degrees (the 5 materials exhibits similar curves and Fig. 9 shows a typical plot calculated from Friedman analysis [22]). This indicates that the decomposition does not take place as a one-step reaction but as multi-step reactions.

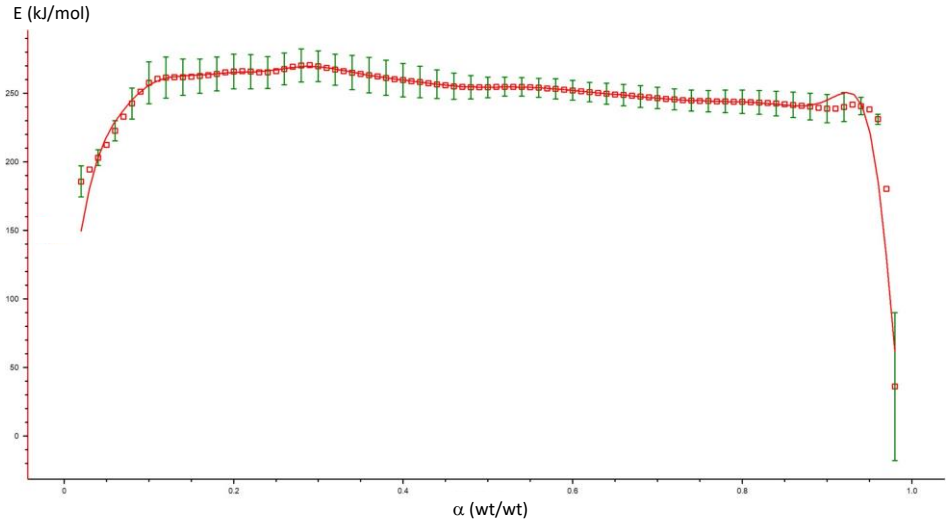

Fig. 9. Typical Friedman plot showing activation energies as a function of conversion degrees (plot for PP-AP760/EG (5:5))

TG curve of neat PP (Fig. 8) showed an apparent single step of decomposition but the Friedman analysis suggested a multi-step of decomposition. The simulation of the curves including only one single step does not give satisfactory results. They were done using reaction models including n-th order function, Avrami-Erofeev function and auto-catalyzed n-th order function but the beginning of the decomposition could not be captured by the model (Fig. 10 (a)). The combination of two successive reactions considering an Avrami-Erofeev function followed by an auto-catalyzed order function gives an excellent fit (Fig. 10 (b)). The number of steps and the resulting calculated kinetic parameters (Table 1) are consistent with the conclusions of the Friedman analysis. The thermal decomposition of PP is a typical radical chain mechanism where initiation, H-abstraction, β-scission and radical recombination reactions are the relevant classes [23]. The first reaction described by an Avrami-Erofeev function (small contribution of about 8% on the whole decomposition) is attributed to chain initiation reactions, which produce radicals and require lower activation energy. The second reaction is attributed to β-scission reactions, which are known to be the main decomposition reactions of PP. The autocatalysis is justified by the formation of allyl radicals and allyl H atoms during the decomposition of PP [24], which can enhance the decomposition of PP. Our reactional scheme makes then sense with the decomposition pathway of PP.

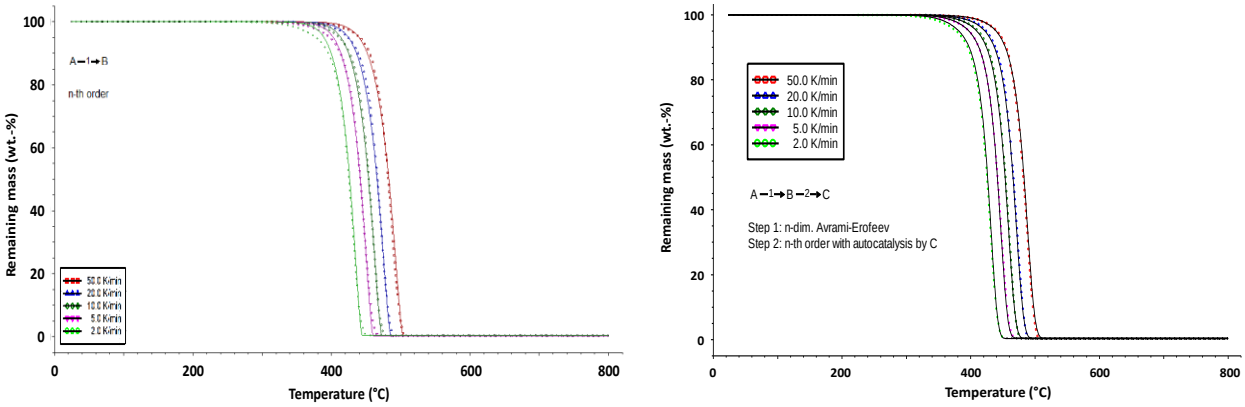

(a) (b)

Fig. 10. Experimental (dots) and simulated (line) TG curves at different heating rates of neat PP fitted with (a) one decomposition step (n-th order function) and (b) with 2 decomposition steps

Intumescence occurs mainly in the condensed phase and it involves numerous chemical reactions. So, kinetic analysis of the reaction in the physical-chemical sense is not possible. That is why we have considered that the overall process of the intumescence could be described by multi-step processes. For the 4 intumescent PPs, TG curves were simulated using the same reactional scheme as the neat PP suggesting the decomposition of the intumescent PPs is mainly governed by the thermal decomposition of the neat PP. The fits are presented using derivative curves to clearly highlight the effect of the assumed reactional scheme (DTG) (Fig. 11). All the fits are excellent and they can capture all the maxima of the DTG curves. It can be then assumed our reactional scheme is appropriate to describe the thermal decomposition of the intumescent materials. The calculated kinetic parameters are shown in Table 1. The activation energies of the intumescent PPs are slightly higher than that of the neat PP indicating some enhancement of the thermal stability of the intumescent PPs.

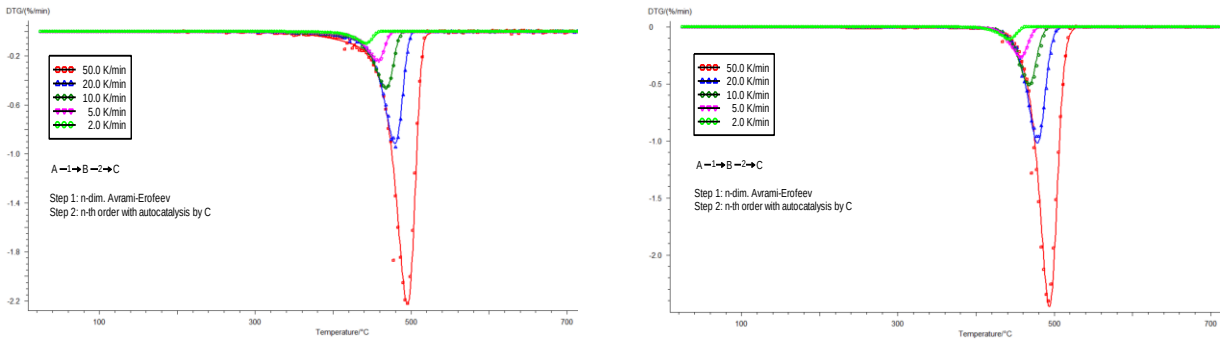

(a) **(b)**

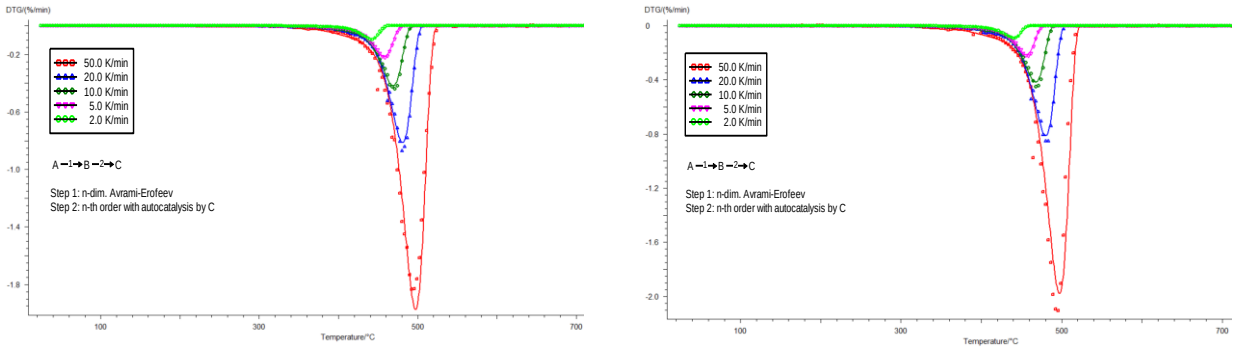

(c) **(d)**

Fig. 11. Experimental (dots) and simulated (line) TG curves at different heating rates of (a) PP-AP760; (b) PP-EG; (c) PP-AP760/EG(5:5) and (d) PP-AP760/EG(9:1).

Table 1. Computed kinetic parameters of the decomposition of neat PP and of the 4 intumescent PPs

Reaction N°	log(A) (A: s^{-1})	E (kJ/mol)	Reaction order or Dimension
PP			
1	11.9 ± 0.3	182 ± 5	0.87 ± 0.07
2	15.3 ± 0.3	245 ± 3	0.91 ± 0.11
PP-AP760			
1	13.5 ± 0.3	204 ± 4	0.53 ± 0.02
2	16.9 ± 0.1	270 ± 2	0.90 ± 0.05
PP-EG			
1	20.4 ± 1.9	260 ± 15	0.20 ± 0.06
2	17.2 ± 0.1	276 ± 2	1.10 ± 0.05
PP-AP760/EG(5:5)			
1	14.9 ± 0.6	219 ± 9	0.58 ± 0.02
2	16.1 ± 0.1	259 ± 2	0.90 ± 0.03
PP-AP760/EG(9:1)			
1	13.3 ± 0.4	205 ± 5	0.53 ± 0.02
2	16.5 ± 0.1	264 ± 2	0.77 ± 0.05

A goal of kinetic analysis is also to simulate the thermal behavior/decomposition of a material. If our assumptions are accurate, we should be able to simulate the decomposition of PP and intumescent PPs in isothermal conditions far from the dynamic conditions used to make our modeling. Thus, to verify the accuracy of our model, the decomposition PP-based materials was simulated in pyrolytic conditions such described as follows:

- Isothermal at 40°C for 10 min (stabilization of the temperature),
- Ramp from 40 to 425°C at 50°C/min,
- Isothermal at 425°C for 120 min.

As it is observed in Fig. 12 in the case of neat PP, the simulated curve fits very well the experimental curve. It means that our approach can be used to simulate the thermal behavior and the pyrolytic decomposition of neat PP. It also validates our model in two successive steps. Note the two-step decomposing model for PP was also recently evidenced by Thiry-Muller using an extended approach of activated complex applied to kinetic analysis [25].

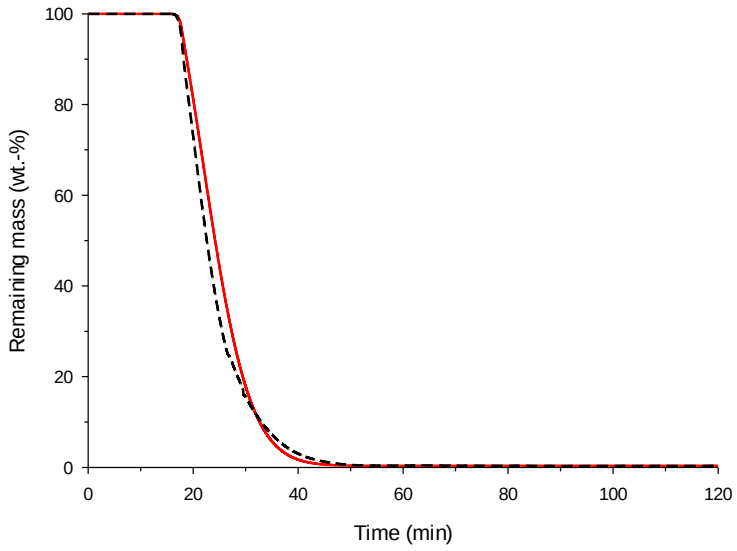

Fig. 12. Experimental (dots) and simulated (line) decomposition curves of neat at 425°C for 120 min (N_2 flow).

The same comparisons were repeated for the intumescent materials (Fig. 13). In all cases, the simulation can capture the decomposition of the materials in isothermal conditions. It supports therefore the selection of the reactional scheme determined for those materials and it gives a series of models for simulating the decomposition of intumescent materials in various conditions.

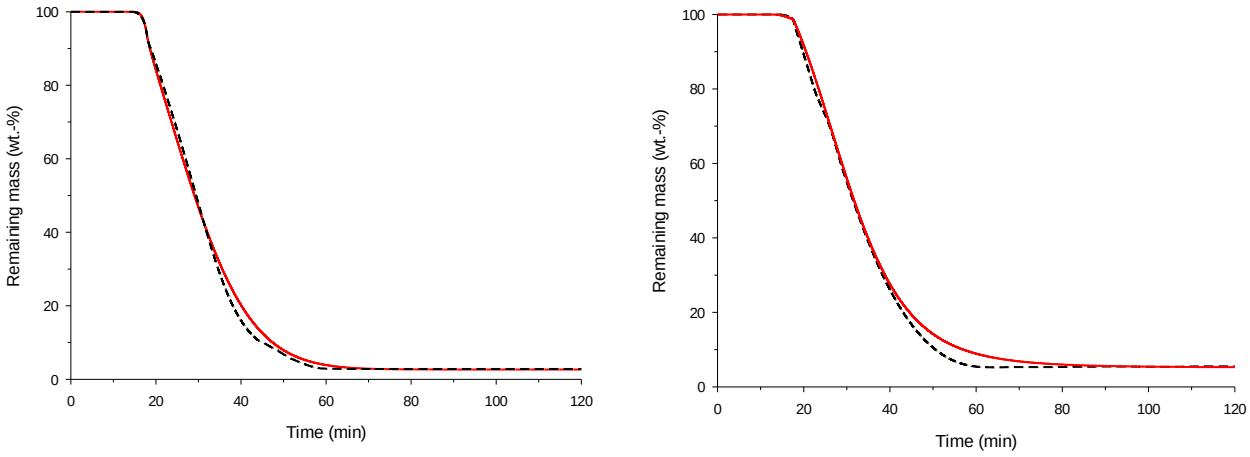

(a) **(b)**

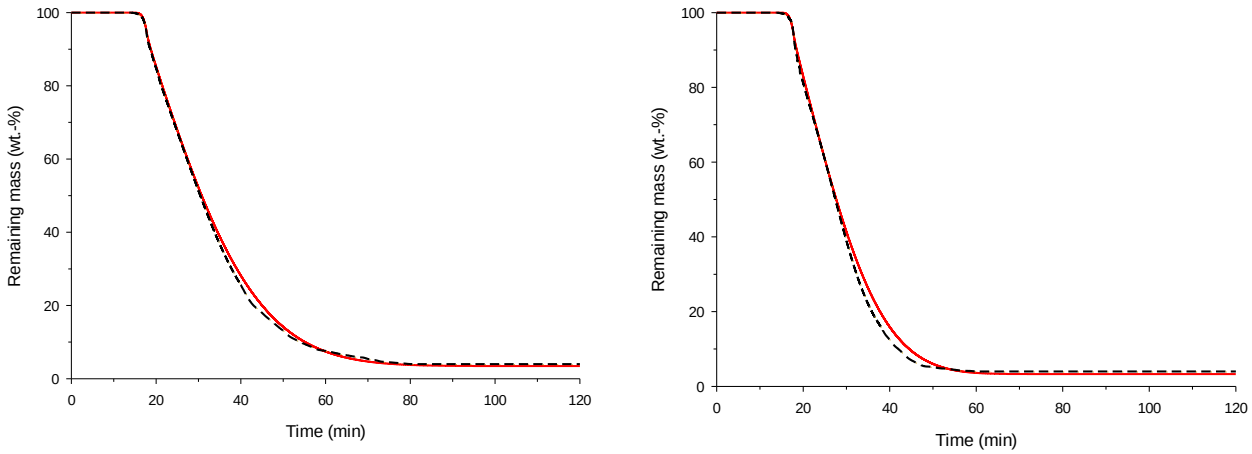

Fig. 13. Experimental (dots) and simulated (line) decomposition curves in isothermal conditions (T = 425°C) of (a) PP-AP760; (b) PP-EG; (c) PP-AP760/EG(5:5) and (d) PP-AP760/EG(9:1).

Fig. 4 showed temperature profiles measured on the backside of the PP-based materials. Two extreme profiles can be distinguished: (i) that of PP-EG exhibiting moderate temperature rise (lowest heating rate of 9°C/min) and (ii) that of PP-AP760/EG(9:1) exhibiting high temperature rise (highest heating rate of 310°C/min). The purpose is then to simulate the decomposition curves of all PP-based materials undergoing the two identified extreme temperature profiles. The simulated curves and the temperature profiles (the curves of temperature profiles were built with linear segments extracted from time/temperature curves of Fig. 4) are shown on Fig. 14. The first profile (low heating rates, Fig. 14 (a)) gives curves exhibiting the same behavior as TG curves already commented for Fig. 8. The second profile (high heating rates, Fig. 14 (b)) shows all PP-based materials decompose in one steep step and all the curves are superimposed (except the char yield, which is the highest at 5 wt.-% for the formulation PP-EG). The decomposition is extremely fast and no further stabilization is provided by the fillers in such conditions. This simulation evidences the incorporated additives do not limit the decomposition rate of PP at high heating rate. It means the intumescent protective coating must be formed rapidly to lower the temperature rise inside the materials and hence, it creates a relatively low heating rate in the materials (creation of large heat gradient in the intumescent coating) and the decomposition of PP can be slowed down. It is consistent with our previous results showing large heat gradient inside the intumescing material and slow temperature rise in the deeper layers of the material [26].

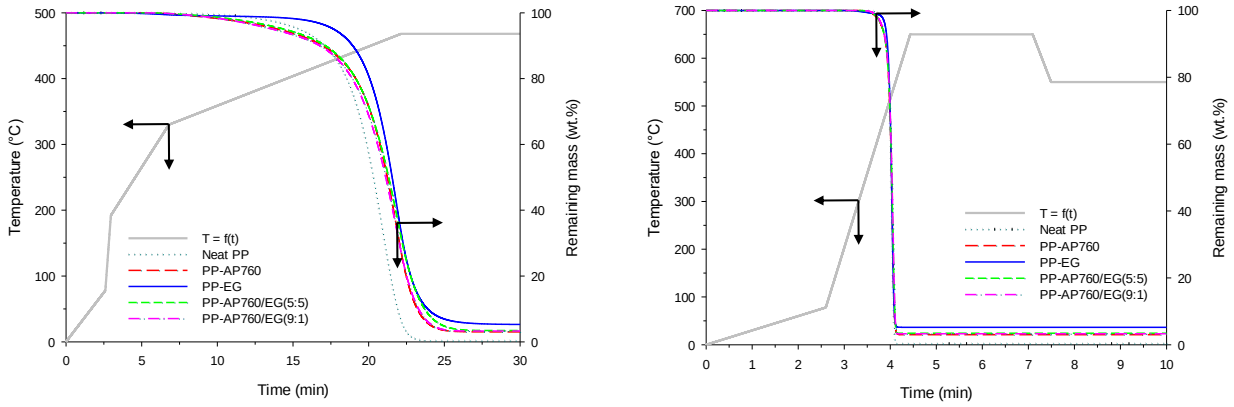

Fig. 14. Simulated decomposing curves of neat PP and intumescent PPs submitting temperature profiles measured on the backside of (a) PP-EG and (b) PP-AP760/EG(9:1) during the cone calorimeter experiment (see Fig. 4).

CONCLUSION

The incorporation of intumescent additives at relatively low loading (10 wt%) in PP permits the reduction by 70% of pHRR. The mode of action occurs via the formation of an expanded carbonaceous layer in all cases. The protective coating acts mainly as heat barrier in the case of the formulations containing AP760 or as heat dissipater with EG. The incorporation of small amount of EG in PP-AP760 modifies heat transfer in the coating creating a strong anisotropy. Upon expansion graphite worms align normal to the surface increasing the transverse heat conductivity (lower efficiency of the heat barrier) and hence, decreasing the fire performance (decrease by only 30% of pHRR). Kinetic analysis done in dynamic conditions on the intumescent PPs permits to determine the kinetic parameters of the decomposition using a reactional scheme at two successive reactions. This model is able to simulate the decomposition of all the materials in isothermal conditions and hence, it can be considered as validated. On the other hand, the kinetic analysis reveals that the intumescent additives do not modify the reactional scheme of the PP thermal decomposition but they increase slightly the thermal stability of the intumescent systems. Further simulations show it could happen only when the heating rate is not too high. Otherwise, the decomposition of the intumescent is the same as that of neat PP.

ACKNOWLEDGEMENT

This work has received funding from the European Research Council (ERC) under the European Union's H2020 – the Framework programme for Research and Innovation (2014-2020) / ERC Grant Agreement n°670747 – ERC 2014 AdG/FireBar-Concept.

REFERENCES

[1] Troitzsch JH, Fires, statistics, ignition sources, and passive fire protection measures, Journal of Fire Sciences, 2016;34: 171-98.
[2] Carty P, Letter to the Editor: Polypropylene Fire at the BASF Plant, Teeside, Fire and Materials, 1996;20: 159-59.
[3] Bourbigot S, Duquesne S, Fire retardant polymers: Recent developments and opportunities, Journal of Materials Chemistry, 2007;17: 2283-300.
[4] Alongi J, Han Z, Bourbigot S, Intumescence: Tradition versus novelty. A comprehensive review, Progress in Polymer Science, 2015;51: 28-73.
[5] Camino G, Costa L, Trossarelli L, Study of the mechanism of intumescence in fire retardant polymers: Part II-Mechanism of action in polypropylene-ammonium polyphosphate-pentaerythritol mixtures, Polymer Degradation and Stability, 1984;7: 25-31.
[6] Morice L, Bourbigot S, Leroy JM, Heat transfer study of polypropylene-based intumescent systems during combustion, Journal of Fire Sciences, 1997;15: 358-74.
[7] Fontaine G, Bourbigot S, Duquesne S, Neutralized flame retardant phosphorus agent: Facile synthesis, reaction to fire in PP and synergy with zinc borate, Polymer Degradation and Stability, 2008;93: 68-76.
[8] Zhu C, He M, Cui J, Tai Q, Song L, Hu Y, Synthesis of a novel hyperbranched and phosphorus-containing charring-foaming agent and its application in polypropylene, Polymers for Advanced Technologies, 2018;29: 2449-56.
[9] Xu B, Wu X, Ma W, Qian L, Xin F, Qiu Y, Synthesis and characterization of a novel organic-inorganic hybrid char-forming agent and its flame-retardant application in polypropylene composites, Journal of Analytical and Applied Pyrolysis, 2018;134: 231-42.
[10] Han L, Wu W, Qi Y, Qu H, Xu J, Synergistic flame retardant effect of BiFeO3 in intumescent flame-retardant polypropylene composites, Polymer Composites, 2017;38: 2771-78.
[11] Dong X, Liu Z, Nie S, Zhang C, Zhou C, Wu W, Synergistic Effects of Novel Intumescent Flame Retardant Polypropylene Composites, Cailiao Yanjiu Xuebao/Chinese Journal of Materials Research, 2017;31: 901-08.
[12] Nie SB, Dong X, Yang JN, Dai GL, Morphology influence of nanoporous nickel phosphate on intumescent flame retardant polypropylene composites, International Polymer Processing, 2018;33: 471-79.
[13] Bourbigot S, Le Bras M, Dabrowski F, Gilman JW, Kashiwagi T, PA-6 clay nanocomposite hybrid as char forming agent in intumescent formulations, Fire and Materials, 2000;24: 201-08.
[14] Bourbigot S, Turf T, Bellayer S, Duquesne S, Polyhedral oligomeric silsesquioxane as flame retardant for thermoplastic polyurethane, Polymer Degradation and Stability, 2009;94: 1230-37.
[15] Focke WW, Badenhorst H, Mhike W, Kruger HJ, Lombaard D, Characterization of commercial expandable graphite fire retardants, Thermochimica Acta, 2014;584: 8-16.
[16] Zheng Z, Liu Y, Zhang L, Wang H, Synergistic effect of expandable graphite and intumescent flame retardants on the flame retardancy and thermal stability of polypropylene, Journal of Materials Science, 2016;51: 5857-71.
[17] Qi F, Tang M, Wang N, Liu N, Chen X, Zhang Z, Zhang K, Lu X, Efficient organic-inorganic intumescent interfacial flame retardants to prepare flame retarded polypropylene with excellent performance, RSC Advances, 2017;7: 31696-706.
[18] Duquesne S, Delobel R, Le Bras M, Camino G, A comparative study of the mechanism of action of ammonium polyphosphate and expandable graphite in polyurethane, Polymer Degradation and Stability, 2002;77: 333-44.
[19] Lu Y, Zhang Y, Xu W, Flame retardancy and mechanical properties of ethylene-vinyl acetate rubber with expandable graphite/ammonium polyphosphate/dipentaerythritol system, Journal of Macromolecular Science, Part B: Physics, 2011;50: 1864-72.
[20] Guo C, Zhou L, Lv J, Effects of expandable graphite and modified ammonium polyphosphate on the flame-retardant and mechanical properties of wood flour-polypropylene composites, Polymers and Polymer Composites, 2013;21: 449-56.
[21] Opfermann J, Kinetic analysis using multivariate non-linear regression. I. Basic concepts, Journal of Thermal Analysis and Calorimetry, 2000;60: 641-58.
[22] Friedman HL, Kinetics of thermal degradation of char-forming plastics from thermogravimetry. Application to a phenolic plastic, Journal of Polymer Science Part C: Polymer Symposia, 1964;6: 183-95.

[23] Lattimer RP, Direct analysis of polypropylene compounds by thermal desorption and pyrolysis-mass spectrometry, Journal of Analytical and Applied Pyrolysis, 1993;26: 65-92.
[24] Ranzi E, Dente M, Faravelli T, Bozzano G, Fabini S, Nava R, Cozzani V, Tognotti L, Kinetic modeling of polyethylene and polypropylene thermal degradation, Journal of Analytical and Applied Pyrolysis, 1997;40-41: 305-19.
[25] Thiry-Muller A. Modélisation de la décomposition thermique des solides. Ph.D. Lemta, University of Lorraine, Nancy, 2018.
[26] Gérard C, Fontaine G, Bellayer S, Bourbigot S, Reaction to fire of an intumescent epoxy resin: Protection mechanisms and synergy, Polymer Degradation and Stability, 2012;97: 1366-86.